The Molecular Arrangement of Membrane-Bound Annexin A2-S100A10 Tetramer as Revealed by Scanning Force Microscopy

Manuela Menke,[a] Michaela Ross,[b] Volker Gerke,[b] and Claudia Steinem*[a]

Annexins are peripheral membrane-binding proteins implicated in a number of membrane-related events (for a review see refs. [1, 2]). Of particular interest within this family is annexin A2, since it can exist in two forms possibly showing different modes of membrane interaction, the annexin A2 monomer and the heterotetrameric complex of annexin A2 with the S100 protein S100A10 (p11). The complex, herein referred to as annexin A2t, is the predominant form of annexin A2 in most cells. It is composed of two annexin A2 molecules linked via their N-terminal domains to a S100A10 dimer.[3] Within the cell, the protein complex is mainly localized to endosomes and at the plasma membrane.[4–6] Recent RNA-interference experiments have revealed a function of the protein in maintaining a proper organization of certain endosomal subdomains.[7,8] In vitro, it has been shown that annexin A2t is capable of binding to negatively charged phospholipids and aggregating chromaffin granules and phospholipid vesicles in a Ca^{2+}-dependent manner (for a review see ref. [9]).

The molecular organization of the junctions between membrane surfaces linked by the annexin A2t complex is still a matter of debate. Two different models have been proposed. The first one is based on electron-density profiles obtained in cryoelectron-microscopy studies.[10,11] It proposes that the dimer of S100A10 is located in the center of the two membranes with one annexin A2 molecule facing the bilayer on each side (Figure 1 A, C).[12] The dimension of the complex between the two membranes was estimated to be 9.0 ± 0.3 nm. The second model assumes that two annexin A2 subunits of the complex are bound to one membrane interface (Figure 1 B).[13] In order to link the two membranes together two heterotetramers then form an octameric structure held together by the S100A10 dimer (Figure 1 D).[14] Bearing these models in mind, two different scenarios are conceivable for an initial Ca^{2+}-dependent binding of annexin A2t to a membrane bilayer. Either one (Figure 1 A) or both annexin A2 subunits (Figure 1 B) of the heterotetramer might bind to the negatively charged phospholipids via Ca^{2+} bridges.

[a] *M. Menke, Prof. Dr. C. Steinem*
Institut für Analytische Chemie, Chemo- und Biosensorik
Universität Regensburg
93040 Regensburg (Germany)
Fax: (+49) 941-943-4491
E-mail: claudia.steinem@chemie.uni-regensburg.de

[b] *Dr. M. Ross, Prof. Dr. V. Gerke*
Institut für Medizinische Biochemie
Zentrum für Molekularbiologie der Entzündung
Westfälische Wilhelms-Universität
von-Esmarch-Straße 56, 48149 Münster (Germany)

 DOI: 10.1002/cbic.200400004

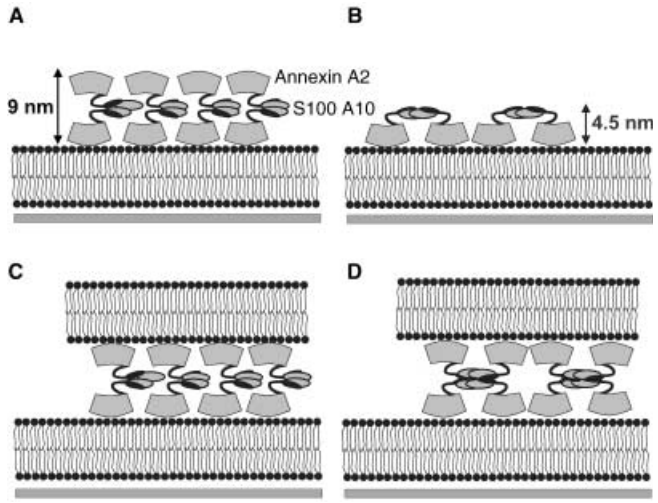

Figure 1. *Schematic illustration of the annexin A2t membrane binding process. A and B show the initial membrane binding, C and D the aggregation process. In the first model (A), the tetrameric complex is bound via one annexin A2 monomer to the membrane. For this arrangement, the resultant height would be about 9 nm for one protein layer. In the second model (B), both annexin subunits of annexin A2t bind to one membrane surface. In this case, an approximate height of about 4.5 nm for one protein monolayer bound to the membrane would be expected. The membrane aggregation process could be mediated by a tetrameric or an octameric structure (C,D).*

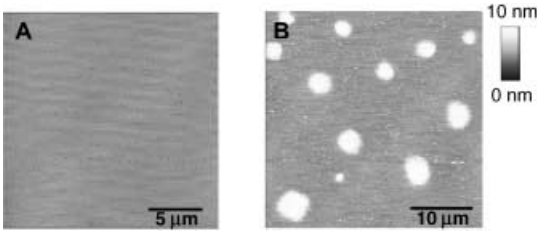

Figure 2. *A) Topographic image of a DPPC–DPPC/DPPS lipid bilayer deposited onto mica by a double Langmuir–Blodgett transfer. B) Topography image after addition of 0.3 μM annexin A2t. The images were obtained in aqueous solution (TRIS/HCl (20 mM), NaCl (100 mM), $CaCl_2$ (1 mM), NaN_3 (1 mM), pH 7.4).*

To elucidate which of the two binding modes is more likely to occur, we determined the height of membrane-bound annexin A2t by scanning force microscopy. Scanning force microscopy on solid-supported Langmuir–Blodgett (LB) bilayers composed of 1,2-dipalmitoyl-*sn*-glycero-3-phosphocholine (DPPC) and 1,2-dipalmitoyl-*sn*-glycero-3-phosphoserine (DPPS) on mica was shown previously to be well suited to visualizing annexin A1 bound to DPPS-enriched domains.[15,16] The method exploits the fact that lipid bilayers composed of DPPC and DPPS are in the gel state at room temperature and are thus only minimally indented during the scanning, thereby reducing the error in the height analysis. The first monolayer of the LB bilayer was composed of DPPC transferred from a water subphase at 45 mN m^{-1}. The second water-exposed monolayer consisted of a mixture of DPPC/DPPS (4:1) transferred at 32 mN m^{-1}. A detailed characterization of these bilayers is given by Ross et al.[15]

Scanning force microscopy (topographic images) of the DPPC-DPPC/DPPS bilayers does not reveal any height differences (Figure 2A) except for some small dark dots, which can be attributed to defects within the bilayers. However, when analyzed by lateral force microscopy, DPPS-enriched domains within the DPPC matrix can be identified in the presence of Ca^{2+} ions (not shown), as shown previously.[15] After addition of 0.3 μM annexin A2t to the immobilized bilayer, round domains, which are 2–5 μm in diameter, become discernable in the topographic images (Figure 2B) and exhibit the same form and distribution as the DPPS-enriched domains as visualized by lateral force microscopy. Thus, we conclude that these higher domains are composed of laterally interacting annexin A2t bound to the DPPS-enriched domains. This result also confirms the specificity of annexin A2t adsorption to acidic phospholipids. Further protein addition did not change the size, number and distribution of the annexin A2t domains. In contrast to the images obtained by Brisson and co-workers for membrane-bound annexin A5,[17,18] in the case of annexin A2t, two-dimensional crystal-like structures could not be resolved by scanning force microscopy. This is in accordance with the results obtained for annexin A1[16] and probably reflects the intrinsic properties of the different annexin proteins analyzed. Reversibility of binding was investigated by addition of a buffer containing 0.1 mM EGTA; this resulted in a complete removal of the protein domains from the membrane. However, nonspecifically bound proteins found in the defects of the membrane, which are visible as small bright dots in the topographic images (Figure 2B), were still present under these conditions and could not be removed by chelating Ca^{2+} (not shown).

The significant topographic contrast between the protein domains and the membrane enabled us to readily obtain an exact height of the protein layer. Figure 3A shows a single domain composed of laterally interacting proteins with a line scan through this domain indicating a height difference between the membrane and the protein layer of 4.3 nm. Histogram analysis of several protein domains ($n = 16$) leads to an average height of 4.2 ± 0.4 nm (see Figure 4A). The two different models outlined above (Figure 1A, B) predict two different but rather well defined heights of the protein layer. For model one (Figure 1A), a height of about 9 nm is expected taking the crystallographic and cryoelectron microscopy data into account.[19] For model two (Figure 1B), the molecular arrangement on top of a phospholipid bilayer would be about 4.5 nm in height. This takes into account that both annexin A2 subunits are bound to the membrane via their convex sides with the S100A10 protruding away from it. Our height analysis is in agreement with the second model and let us conclude that in a first step the annexin A2 tetrameric complex binds to a model membrane simultaneously with both annexin A2 subunits. The slightly smaller value of 4.2 nm might be explained by the fact that the protein coverage on the surface is always less than one and the height is determined as an average value of a certain area, so that the measured height is expected to be slightly smaller than that of a single protein.

To corroborate our results, we also investigated by scanning force microscopy the height of membrane-bound monomeric

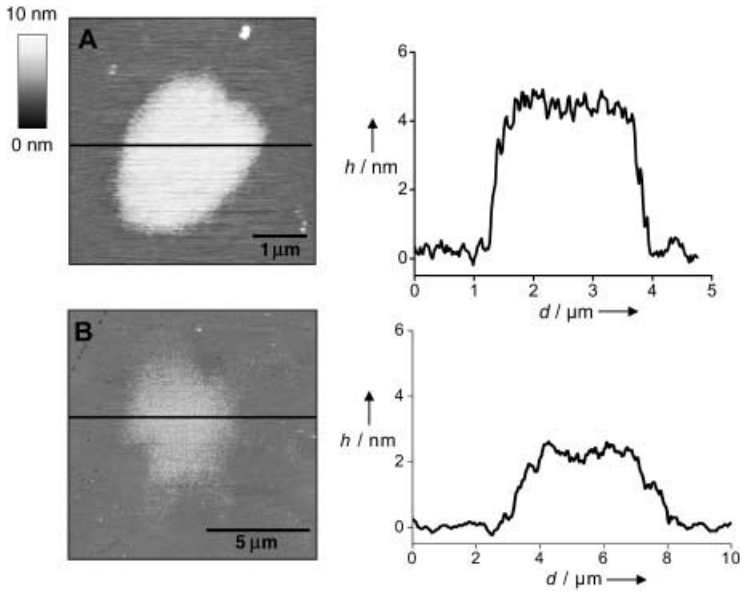

Figure 3. *Topographic image of A) an annexin A2t and B) an annexin A2 monomer protein domain. The black lines indicate the corresponding line scan with the height profiles depicted on the right-hand side. The difference between the lipid bilayer and the protein layer is 4.3 nm for the tetrameric complex. The cross section for the annexin A2 monomer protein domain indicates a height difference of 2.5 nm. All images were obtained in aqueous solution (TRIS/HCl (20 mM), NaCl (100 mM), $CaCl_2$ (1 mM), NaN_3 (1 mM), pH 7.4).*

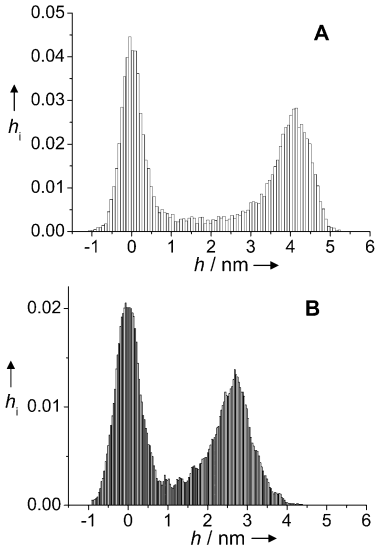

Figure 4. *Typical height-analysis histogram of A) an annexin A2t and B) an annexin A2 monomer protein domain. Two well-separated frequency peaks are observed, which are assigned to the lipid layer (set to zero) and the protein. The height difference is calculated as the difference between the two peak maxima and was determined to be 4.1 nm for the annexin A2 heterotetramer and 2.8 nm for the annexin A2 monomer.*

annexin A2. Monomeric annexin A2 was obtained by dissociating the heterotetrameric complex in urea followed by size-exclusion chromatography to separate the individual subunits, which were renatured individually.[20] Successful renaturation of annexin A2 was confirmed by verifying its typical Ca^{2+}-dependent binding to negatively charged phospholipids. Addition of the annexin A2 monomer to a DPPC–DPPC/DPPS bilayer again leads to round protein domains of similar size to those obtained by binding annexin A2t (Figure 3B). Histogram analysis of the annexin A2 monomer domains reveals a height for the protein layer of 2.8 ± 0.7 nm ($n = 8$; Figure 4B). This value is similar to the one obtained for monomeric annexin A1 bound to DPPC–DPPC/DPPS bilayers (3.1 ± 0.2 nm),[16] but is much lower than that obtained for the tetrameric complex. The height of about 3 nm for membrane-bound monomeric annexin A2 agrees with the crystallographic data for the annexin A2 core.[19] The difference between monomeric and tetrameric annexin A2 is about 1.4 nm and can be attributed to the S100A10 dimer. Related S100 dimers such as calcyclin and calbindin 9k exhibit dimensions of about $3.8 \times 3.3 \times 3.1$ nm[21] and $2.5 \times 3.0 \times 3.0$ nm,[22] respectively. The predicted dimensions of S100A10 dimers of about 3 nm imply that the S100A10 molecules could be arranged next to each other in the manner shown in Figure 1B; this would result in a height difference between monomeric annexin A2 and the heterotetrameric complex of around 1.5 nm.

As the Ca^{2+}-dependent membrane binding of the annexin core is a dynamic process, two possible scenarios could account for the aggregation initiated by annexin A2t. The first one is depicted in Figure 1C, where the junction between the two membranes involves single annexin A2t molecules connecting the surfaces of opposing membranes. This arrangement is favored by electron-density profiles obtained by cryoelectron microscopy and model calculations.[11,12] Since our data indicate that in the initial membrane binding event both annexin A2 molecules are bound to one membrane interface, desorption and rebinding to the opposing membrane of one of the two annexin A2 subunits of the complex has to occur. In the second model (Figure 1D) the membrane aggregation is mediated by protein–protein interactions; this results in an octameric annexin A2–S100A10 complex. This molecular arrangement was favored by Waisman in the case of annexin A2t–chromaffin granules interactions[13] and has also been discussed to occur following disulfide-bridge formation between cysteines within the C-terminal region of S100A10.[14] Future experiments employing scanning force microscopy and analyzing the topography of annexin A2-S100A10 complexes assembled from individual subunits on DPPC–DPPC/DPPS bilayers should resolve this issue.

Experimental Section

Materials: DPPC and DPPS were purchased from Avanti Polar Lipids (Alabaster, AL, USA) and used without further purification. Annexin A2t was purified from porcine intestinal epithelium according to Gerke and Weber.[23] Protein concentration was determined by UV absorption with $\varepsilon_{280\,nm} = 0.65\ cm^2\,mg^{-1}$. Protein purity was analyzed by SDS-PAGE. Monomeric annexin A2 was isolated from the tetrameric complex. After denaturation in 9 M buffered

urea, the annexin A2 and S100A10 subunits were separated by size-exclusion chromatography.[20] Subsequent dialysis against TRIS/HCl (20 mM), NaCl (100 mM), NaN_3 (1.5 mM), $MgCl_2$ (2 mM), DTT (0.5 mM), pH 7.5 yielded the renaturated proteins. Purity was analyzed by SDS-PAGE, and protein concentration was determined by UV absorption with $\varepsilon_{280\,nm} = 0.75\ cm^2\,mg^{-1}$.

Lipid-bilayer preparation: Lipid bilayers were prepared by the Langmuir–Blodgett technique. LB films were prepared at 20 °C from the air/water interface on a film balance equipped with a Wilhelmy plate (Riegler–Kirstein, Golm, Germany) with the help of a dipper device. The Teflon trough was 175.5 cm^2. As subphase, ultrapure water was used. After being spread, the lipid film was equilibrated for 30 min. The first monolayer composed of DPPC was compressed to a surface pressure of 45 $mN\,m^{-1}$, equilibrated again for 30 min, and was then deposited on a freshly cleaved mica plate maintaining the surface pressure constant. A second monolayer composed of DPPC/DPPS (4:1) was transferred on top of the DPPC monolayer at a surface pressure of 32 $mN\,m^{-1}$.[15]

Scanning force microscopy (SFM): Surface images were obtained in an open Teflon fluid chamber with a JPK NanoWizard scanning force microscope (JPK Instruments, Berlin, Germany). Measurements were performed in TRIS/HCl (20 mM), NaCl (100 mM), $CaCl_2$ (1 mM), NaN_3 (1 mM), pH 7.4. Protein was added from a stock solution to the fluid chamber with 1 mL volume to final concentrations of 0.3 μM for annexin A2t and 0.6 μM for annexin A2 monomer. Images were obtained in contact or intermitted-contact mode, respectively, by using microfabricated silicon nitride tips (NP-S, Digital Instruments, Santa Barbara, CA, USA) or silicon tips (CSC37/50 E, Ultrasharp, Silicon-MDT Ltd., Moscow, Russia). For the contact mode, V-shaped cantilevers with a nominal spring constant of 0.32 $N\,m^{-1}$ were used, while for intermitted contact mode, cantilevers with nominal spring constants of 0.3 $N\,m^{-1}$ and resonant frequencies of 21 kHz were employed. Usual scan rates were set to 0.3 Hz. Image resolution was 512×512 pixels.

Acknowledgements

Financial support by the DFG (graduate college 760) was gratefully acknowledged.

Keywords: annexins · lipid bilayers · membrane proteins · protein domains · scanning probe microscopy

[1] V. Gerke, S. E. Moss, *Physiol. Rev.* **2002**, *82*, 331–371.
[2] P. Raynal, H. B. Pollard, *Biochim. Biophys. Acta* **1994**, *1197*, 63–93.
[3] S. Rety, J. Sopkova, M. Renouard, S. Tabares, D. Osterloh, V. Gerke, F. Russo-Marie, A. Lewit-Bentley, *Nature Struct. Biol.* **1999**, *6*, 89–95.
[4] L. Zokas, J. R. Glenney, Jr., *J. Cell Biol.* **1987**, *105*, 2111–2121.
[5] C. Thiel, M. Osborn, V. Gerke, *J. Cell. Sci.* **1992**, *103*, 733–742.
[6] S. Chasserot-Golaz, N. Vitale, I. Sagot, B. Delouche, S. Dirrig, L. A. Pradel, J. P. Henry, D. Aunis, M. F. Bader, *J. Cell Biol.* **1996**, *133*, 1217–1236.
[7] N. Zobiack, U. Rescher, C. Ludwig, D. Zeuschner, V. Gerke, *Mol. Biol. Cell* **2003**, *14*, 4896–4908.
[8] N. Mayran, R. G. Parton, J. Gruenberg, *EMBO J.* **2003**, *22*, 3242–3253.
[9] C. E. Creutz, *Science* **1992**, *258*, 924–931.
[10] O. Lambert, N. Cavusoglu, J. Gallay, M. Vincent, J. L. Rigaud, J.-P. Henry, J. Alaya-Sanmartin, *J. Biol. Chem.* **2004**, *279*, 10872–10882.
[11] O. Lambert, V. Gerke, M. F. Bader, F. Porte, A. Brisson, *J. Mol. Biol.* **1997**, *272*, 42–55.
[12] J. Sopkova-de Oliveira Santos, F. K. Oling, S. Rety, A. Brisson, J. C. Smith, A. Lewit-Bentley, *Biochim. Biophys. Acta* **2000**, *1498*, 181–191.
[13] D. M. Waisman, *Mol. Cell. Biochemistry* **1995**, *149/150*, 301–322.
[14] A. Lewit-Bentley, S. Rety, J. Sopkova-de Oliveira Santos, V. Gerke, *Cell. Biol. Int.* **2000**, *24*, 799–802.
[15] M. Ross, C. Steinem, H.-J. Galla, A. Janshoff, *Langmuir* **2001**, *17*, 2437–2445.
[16] A. Janshoff, M. Ross, V. Gerke, C. Steinem, *ChemBioChem* **2001**, *2*, 587–590.
[17] I. Reviakine, W. Bergsma-Schutter, D. Mazeres-Dubut, N. Govorukhina, A. Brisson, *J. Struct. Biol.* **2000**, *131*, 234–239.
[18] I. Reviakine, W. Bergsma-Schutter, A. Brisson, *J. Struct. Biol.* **1998**, *121*, 356–361.
[19] A. Burger, R. Berendes, S. Liemann, J. Benz, A. Hofmann, P. Gottig, R. Huber, V. Gerke, C. Thiel, J. Romisch, K. Weber, *J. Mol. Biol.* **1996**, *257*, 839–847.
[20] V. Gerke, K. Weber, *J. Biol. Chem.* **1985**, *260*, 1688–1695.
[21] B. C. Potts, J. C. Smith, M. Akke, T. J. Macke, K. Okazaki, H. Hidaka, D. A. Case, W. J. Chazin, *Nature Struct. Biol.* **1995**, *2*, 790–796.
[22] D. M. E. Szebenyi, S. K. Obendorf, K. Moffat, *Nature Struct. Biol.* **1981**, *294*, 327–332.
[23] V. Gerke, K. Weber, *EMBO J.* **1984**, *3*, 227–233.

Received: January 12, 2004

